As originally published in the International Conference on Soldering and Reliability Preedings.

A GEOMETRY AND SIZE INDEPENDENT FAILURE CRITERION FOR FRACTURE PREDICTION IN LEAD-FREE SOLDER JOINTS

Siva P. V. Nadimpalli and Jan K. Spelt
Department of Mechanical and Industrial Engineering
University of Toronto
Toronto, ON, Canada
spelt@mie.utoronto.ca

ABSTRACT
Solder joint fracture due to mechanical loads, such as drop impact and board bending, is a significant reliability concern, but little attention has been paid to the development of methods of predicting solder joint fracture under such loading conditions. This paper evaluates a failure criterion that can predict joint failure independent of joint size and geometry. In the first part of the work, continuous and discrete SAC305 solder joints of different lengths were made between copper bars using standard surface mount processing conditions, and then fractured under various loading combinations: pure tensile stress, mixed tensile and shear stress. The critical loads corresponding to crack initiation in the continuous joints were measured and used to determine the fracture parameters at initiation, G_{ci} and J_{ci}. This serves as a strength property for the solder-substrate system. In the second part of the investigation, fracture of discrete solder joints was simulated using elastic and elastic-plastic finite element methods, and crack initiation was predicted using the measured G_{ci} and J_{ci} values for this solder system. The predictions matched reasonably well with the measured values. An interesting observation was that the failure of joints less than 2 mm in length can be predicted using the fracture parameters at initiation from continuous joints. This suggests that G_{ci} and J_{ci} measured in this way should also provide a strength property that is applicable to failure prediction in much smaller microelectronic joints. In fact, some preliminary fracture predictions of solder balls in a PBGA package showed a good agreement with experimental observations. The scope of this study was limited to quasi-static loading, but the methodology can be extended to impact and high-temperature loading conditions.

Keywords: lead-free solder, fracture prediction, finite element analysis, PBGA

INTRODUCTION

Solder joint failure under mechanical loading such as drop impact and vibration is of great interest, but relatively little attention has been paid to the development of methods to predict the fracture load of solder joints under quasi-static mechanical loads, applied either directly on components or induced by the bending or twisting of printed circuit boards (PCBs).

Existing experimental methods to evaluate the strength of solder joints such as ball shear [1, 2], ball pull [3], board level bending [4], and board level drop tests [5,6] are useful mainly for quality control and not for failure prediction since they depend on the details of the test. For example, Tan et al. [7] have proposed a force-based failure criterion by measuring the strength of individual 500 μm Sn-Pb solder balls subjected to different combinations of normal and shear loads and creating a force-based failure envelope. Using this criterion they were able to predict the failure of solder joints in a board level bending test. However, the limitations of this type of force-based prediction method are similar to those of the previously mentioned quality control tests; i.e. force-based criteria are applicable only to the particular type of joint and loading for which the force envelope was developed (e.g. a 500 μm solder ball in [7]).

Fracture-based criteria such as the critical energy release rate G_c and J-integral as a function of the mode ratio of loading [8, 9, 10] have been used widely to predict failure in adhesive joints. Some attempts have been made [11, 12] to use these fracture criteria to predict the strength of solder joints.

The present study examined the applicability of the solder joint fracture initiation criteria G_{ci} and J_{ci} that would permit the prediction of solder joint strength for a wide range of joint geometries and types of load (i.e., combinations of tensile and shear loads). DCB specimens made with a continuous Cu-SAC305 solder layer were fractured under mode-I and mixed-mode loading to measure the initiation fracture properties G_{ci} and J_{ci}. Using these properties in subsequent finite element simulations, fracture loads of discrete solder joints arranged in a linear array between two copper bars were predicted, and the predictions were compared with experimental data to evaluate the failure criteria. Finally, some preliminary predictions of solder ball fracture in a PBGA package loaded under three-point bending were made.

EXPERIMENTAL METHODS

Double cantilever beam (DCB) specimens made with either a continuous solder joint (Fig.1a) or discrete l=2 mm and 5 mm joints (Fig.1b) were used in the fracture experiments. The specimens consisted of two copper bars joined with a 0.4 mm thick Sn3.0Ag0.5Cu (SAC305) solder joints. The processing conditions were typical of surface mount

manufacturing conditions so that the specimens had microstructures similar to those of commercial BGA joints [13].

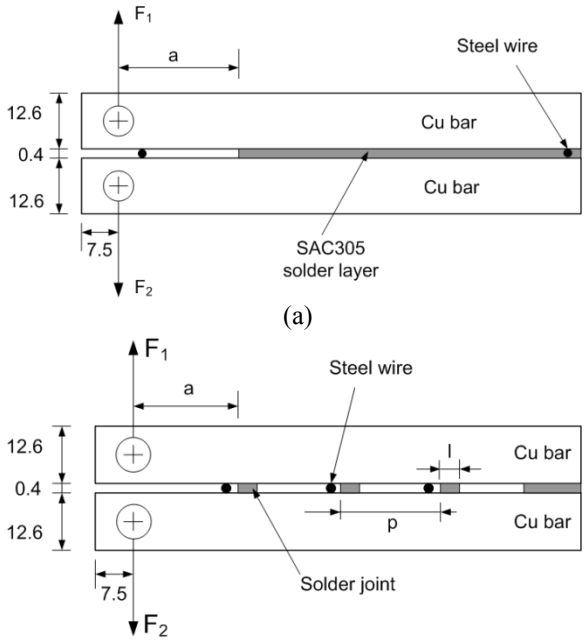

Fig. 1 Schematic of a) the continuous joint DCB specimen and b) discrete solder joint specimen (l=2 mm and 5 mm). The width of the specimen was 12.6 mm and overall length was 160 mm. All dimensions in mm.

These specimens were fractured under mode-I (tensile) and various mixed-mode (combined tensile and shear loading) conditions using a load jig that enables the forces on the DCB arms to be varied independently resulting in a range of mode ratios [14]. The tests were conducted under displacement control at a cross-head speed of 0.1 mm/min. The loading on the Cu bars continued until crack initiation was observed using a microscope with a field of view of approximately 1.9 mm. More details about these tests can be found in [12].

FINITE ELEMENT MODELS

The fracture parameters at crack initiation, J_{ci} and G_{ci}, were calculated from the specimen properties and the measured initiation loads using 2D elastic-plastic and elastic finite element models, respectively. Figure 2 shows the mesh and boundary conditions of a continuous joint DCB specimen. The Cu bars were modeled using plane stress and the solder layer using plane strain PLANE183 elements available in ANSYS© 12 finite element software [15]. These elements are efficient for fracture modeling. Similar mesh details were used in the modeling of the discrete joints.

The elastic strain energy release rate, G, and phase angle, ψ, were obtained as

$$G = (1-\nu^2)\left(\frac{K_{II}^2 + K_I^2}{E}\right) \quad (1)$$

and

$$\psi = \arctan\left(\frac{K_{II}}{K_I}\right), \quad (2)$$

where K_{II} and K_I are mode-II and mode-I stress intensity factors, respectively, obtained from ANSYS for the given boundary conditions. The E and ν are the Young's modulus and Poisson's ratio of SAC305 solder, respectively. The elastic-plastic fracture parameter, J-integral, was obtained directly from FE model for four different paths surrounding the crack tip for the given load and displacement boundary conditions. As expected, the J-integral values for these paths were almost same, and an average value was used as the strain energy release rate [12].

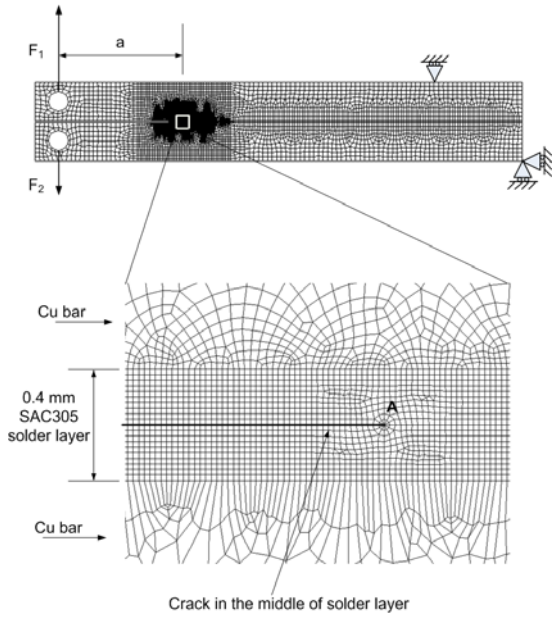

Fig. 2 Finite element mesh of the DCB specimen showing the overall view with boundary conditions and the details near the crack tip, denoted as A [12].

RESULTS AND DISCUSSION

Crack Initiation in Continuous Joint DCB Specimens

The measured crack initiation loads of continuous DCBs under mode-I and the mixed-mode conditions were used to calculate the fracture parameters at initiation, G_{ci} and J_{ci}, using the elastic and elastic-plastic finite element models, respectively. Figure 3 shows that G_{ci} increased with phase angle, from an average G_{ci}=480 J/m^2 in mode I to 700 J/m^2 at ψ=45°. This dependence on the mode ratio is attributed to the larger plastic zone near the crack tip at higher phase angles due to the presence of shear [16]. Also, note that for $\psi \leq 25°$, G_{ci} and J_{ci} were both approximately 480 J/m^2, but diverged as the mode ratio increased; e.g. at ψ =45°, the elastic model resulted in G_{ci} =700 J/m^2, whereas the elastic-plastic model resulted in J_{ci}=820 J/m^2. This deviation can be attributed to the increasing amount of plastic dissipation

at higher mode ratios, which was not captured by the elastic model. Hence, the fracture parameter J_{ci} was used to predict fracture of the discrete joints at higher mode ratios.

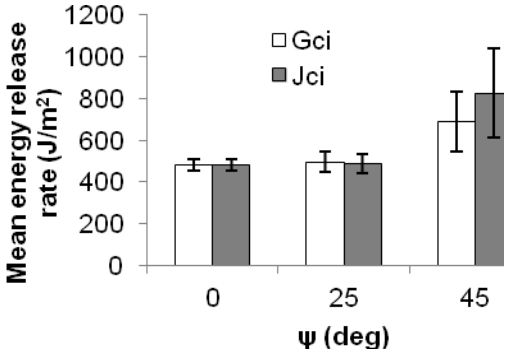

Fig. 3 Comparison of mean initiation energy release rates, G_{ci} and J_{ci}, as a function of phase angle of continuous joint DCB specimens [12].

Predicting Mode-I Crack Initiation Loads in Discrete 2 mm and 5 mm Solder Joints

Figures 4 and 5 show the failure loads of l=2 mm and l= 5 mm joints in several specimens tested under mode-I loading as a function of the loading arm length (a in Fig. 1). These loads were predicted using the mode-I G_{ci} of continuous joint DCBs [11]. It can be seen that the predictions of the FE model (solid curve) were very close, and agreed reasonably well with experiments.

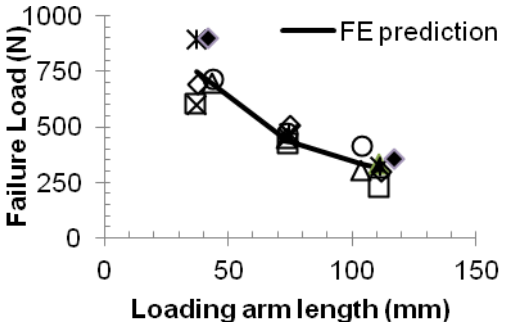

Fig. 4 Measured mode-I crack initiation loads for eight specimens with l=2 mm and predictions based on the G_{ci} value of continuous DCBs. The symbols represent experimental data from different specimens [11]. The loading arm length is distance a in Fig. 1b.

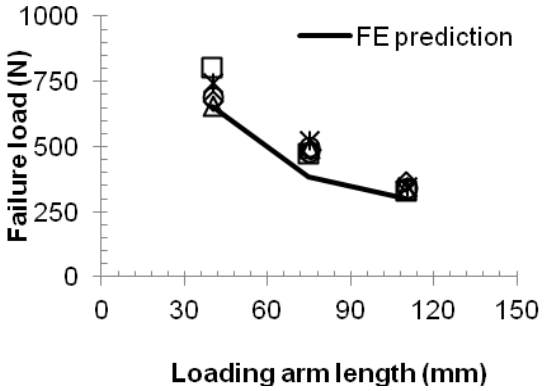

Fig. 5 Measured crack initiation loads for six specimens with l=5 mm tested under mode-I and predictions based on the G_{ci} from continuous DCB. The symbols represent experimental data from the different specimens [11]. The loading arm length is distance a in Fig. 1b.

Mixed-mode Fracture Predictions in Discrete 2 mm Solder Joints

The average J_{ci} (ψ) calculated using the FEA at the measured crack initiation loads for the continuous DCB joints was compared with the J_{ci} values calculated from the initiation loads of the discrete l=2 mm joints in Fig. 6. It is noted that they both follow the same trend with respect to the phase angle, and the average J_{ci} from the continuous DCB provides a lower bound strength prediction for the discrete joints. Similar observations were made in the case of l=5 mm discrete joints [12].

Strain Energy Release Rate as a Fracture Criterion

It was observed in the earlier sections that the strain energy release rate at crack initiation from continuous DCBs can be used to predict the failure of the smaller joints. In fact, the predictions based on the mean initiation fracture properties G_{ci} and J_{ci} from continuous DCBs at various mode ratios was within 14% for l=2 mm and l=5mm joints (Figs. 4, 5 and 6). Therefore, the J_{ci} (ψ) solder crack initiation criterion can be used for different joint geometries under various mixed-mode conditions to predict the failure loads of the smaller joints.

Although these predictions pertain to quasi-static loading conditions, this methodology can be extended to fracture under high strain-rate and higher temperature conditions; however, the strength properties (i.e. J_{ci}) would have to be measured under these conditions.

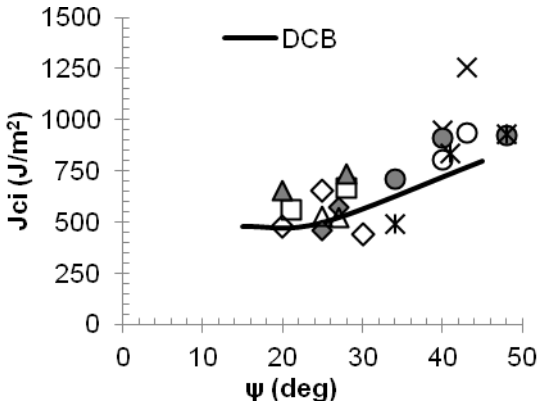

Fig. 6 The initiation energy release rate, J_{ci}, of discrete l=2 mm joints as a function of phase angle from nine specimens (i.e., symbols) is compared with the average J_{ci} values obtained from continuous joint DCBs (i.e., solid curve) [12].

Application of J_{ci} (ψ) Criterion for Prediction of SAC Solder Ball Fracture in a PBGA Package: Preliminary Results

Three-Point Bending Experiments

The PBGA256 package of 27 mm length size and 1.27 mm pitch with SAC405 solder ball was considered. The PCB finish was immersion Ag. The test specimen shown in Fig. 7 was cut from the package and PCB assembly, such that a 4x4 array of solder balls remained at each end of the package. The specimen was tested in three-point bending (Fig. 8).

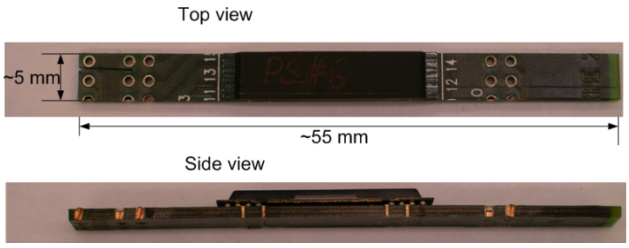

Fig. 7 A typical specimen obtained from a PBGA256 package of 27mm x 27mm size with a pitch of 1.27mm. The solder ball is made of SAC405 lead free alloy.

Figure 9 shows the load displacement response of PBGA specimens from four different experiments. The lower slope of the curve to 1 mm was due to the clearance of the loading train and sliding of the specimen. The reaction force of the specimen increased almost linearly with displacement until the first row of solder balls started cracking. The load at the onset of fracture in the first row of balls and at their break was almost the same as indicated by the first peak in each curve, approximately at 23 N force and 2.3 mm deflection. It was observed that the identification of the onset of fracture was possible from this load displacement response, because this failure created a significant stiffness change in the sample (peak in Fig. 9). The crack initiation was additionally confirmed with a microscope. With further increase in the displacement, the reaction force increased with a slightly lower slope than before while the subsequent row of balls was fractured. However, it was not possible to identify their fracture load accurately from this curve alone.

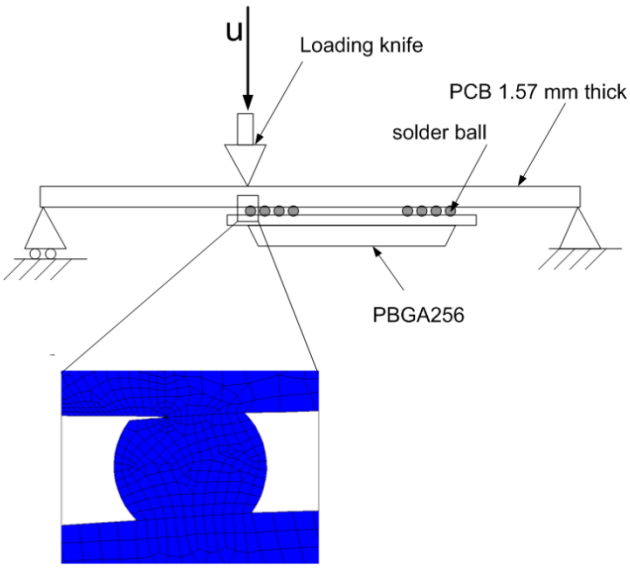

Fig. 8 Schematic of three-point bending experiment of PBGA package. The zoomed view shows finite element mesh near the critically loaded solder joint. A crack was modeled at the interface between PCB and solder as per the experimental observation.

The three-point bending experiment shown in Fig. 8 was then simulated using ANSYS software with a 2D plane strain simplification. The mechanical properties for the package and PCB were obtained from [17]. The calculated J-integral for 2.3 mm deflection, which was the crack initiation point (Fig. 9) in a BGA ball, was approximately 980 J/m^2 and the corresponding phase angle was 38°. From Figs. 3 and 6 and Table 1, it can be noted that the J_{ci} of the SAC305 DCB at ψ=38° was approximately 800 J/m^2; i.e. 22% lower than the predicted critical value, J_{ci}=980 J/m^2. This discrepancy can be expected because of the 2D simplification in the FEA which may not represent the actual 3D stress state in a BGA ball accurately. In addition, the PBGA package had SAC405 solder with an Ag finish, which might have a slightly different characteristic J_{ci}(ψ) compared to the SAC305 solder joint with an OSP finish (i.e., Figs. 3 and 6). Unfortunately, the fracture initiation data for SAC405 solder with Ag substrate finish was not available. Further work is under way with PBGA samples made with SAC305 and an OSP finish, consistent with the available J_{ci} data of Figs. 3-5. Hence, this result (Table 1) indicates that the J_{ci} (ψ) criterion holds promise as a means to predict the failure in solder joints of the size of BGA solder balls.

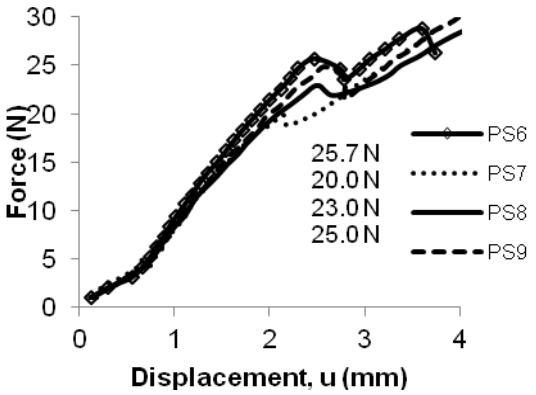

Fig. 9 Load displacement response of PBGA256 package in three-point bending experiment. Data from four experiments.

Table 1 Comparison of solder ball J_{ci} in three-point bending with continuous DCB J_{ci}.

	Three-point bending of PBGA	DCB (Figs.3 and 6)	% difference
J_{ci} (J/m^2) at ψ=38°	980	~800	22

The prediction methodology demonstrated in this study has some practical advantages. The strength property J_{ci} (ψ) can be obtained from relatively simple fracture experiments with DCB specimens, and this property should be applicable to solder joints in other electronic packages, not just BGAs. Moreover, its calculation in solder joints using FEA is much less sensitive to modeling details than is the prediction of maximum stress or strain.

CONCLUSIONS

The copper bar DCB specimens made with continuous SAC305 solder layesr were fractured under pure tensile and various combinations of tensile and shear loads to measure the characteristic fracture energies corresponding to crack initiation, G_{ci} and J_{ci}. Using these fracture properties as a failure criterion, crack initiation loads in discrete 2 mm and 5 mm long joints under different loading combinations were predicted with finite element models. These loads were then compared with experimental data and the predictions agreed to within 14%. The same fracture criterion was then extended to predict the fracture of solder balls in a PBGA package with SAC405 tested under three-point bending. The predictions agreed reasonably well with experimental observations, considering that J_{ci} for SAC405 was estimated from the value for SAC305.

ACKNOWLEDGEMENTS

The authors gratefully acknowledge the advice and assistance of Polina Snugovsky of Celestica Inc., and Laura Turbini, Bev Christian and Gene Burger of Research in Motion Inc. The research was supported by funds from these companies as well as the Ontario Centres of Excellence and the Natural Sciences and Engineering Research Council of Canada.

REFERENCES

[1] Kim JW, Jung SB. Experiment and finite element analysis of the shear speed effects on the Sn-Ag and Sn-Ag-Cu BGA solder joints. Mater Sci Eng A 2004; 371:267-76.

[2] JESD 22-B117A, JEDEC Solid State Technology Association, Arlington, VA, USA, 2006.

[3] Newman K. BGA brittle fracture- Alternative solder joint integrity test methods. Electron Comp Tech Conf, 2005, p. 1194-201.

[4] Seah SKW, Wong EH, Mai YW, Rajoo R, Lim CT. High-speed bend test method and failure prediction for drop impact reliability. Electron Comp Tech Conf, 2006, p.1003-08.

[5] Chong DYR, Che FX, Pang JHL, Ng K, Tan JYN, Low TH. Drop impact reliability testing for lead-free and lead based soldered IC packages. Microelectron Reliab 2006; 46:1160-71.

[6] JESD22-B111, JEDEC Solid State Technology Association, Arlington, VA, USA, 2003.

[7] Tan LB, Xiaowu Z, Lim CT, Tan VBC. Mapping the failure envelope of board-level solder joints. Microelectron Reliab 2009; 49:397-409.

[8] Fernlund G, Spelt JK. Failure load prediction of structural adhesive joints. Part 1: analytical method. Int J Adhes Adhes 1991; 11(4):213–20.

[9] Fernlund G, Spelt JK. Mixed mode energy release rates for adhesively bonded beam specimens. J Comp Tech Res 1994;16(3):234–43.

[10] Azari S, Eskandarian M, Papini M, Schroeder JA, Spelt JK. Fracture load predictions and measurements for highly toughened epoxy adhesive joints. Engng Fract Mech 2009; 76:2039–55.

[11] Nadimpalli SPV, Spelt JK. Fracture load predictions of lead-free solders. Submitted to Engng Fract Mech 2010.

[12] Nadimpalli SPV, Spelt JK. Mixed-mode fracture load predictions of lead-free solders. Manuscript in preparation.

[13] Nadimpalli SPV, Spelt JK. R-curve behavior of Cu–Sn3.0Ag0.5Cu solder joints: Effect of mode ratio and microstructure. Mater Sci Eng A 2010; 527:724-34.

[14] Fernlund G, Spelt JK. Mixed-mode fracture characterization of adhesive joints. Comp Sci Technol 1994; 50: 441-9.

[15] ANSYS® Academic Research, Release 12.0 Documentation, 2009, ANSYS Inc. Canonsburg, PA, United States.

[16] Hutchinson JW, Suo Z. Mixed mode cracking in layered materials. Adv. Appl. Mech, J.W. Hutchinson and T.Y.Wu Eds. New York: Academic 1992; 29: 63-191.

[17] Liu X, Sooklal VK, Verges MA, Larson MC. Experimental study and life prediction on high cycle.
vibration fatigue in BGA packages. Microelectron Reliab 2006: 46;1128–38.